HAL open science

System identification of MISO fractional systems: Parameter and differentiation order estimation

Stéphane Victor, Abir Mayoufi, Rachid Malti, Manel Chetoui, Mohamed Aoun

To cite this version:

Stéphane Victor, Abir Mayoufi, Rachid Malti, Manel Chetoui, Mohamed Aoun. System identification of MISO fractional systems: Parameter and differentiation order estimation. Automatica, 2022, 141, pp.110268. 10.1016/j.automatica.2022.110268 . hal-03722681

HAL Id: hal-03722681

https://hal.science/hal-03722681v1

Submitted on 16 Oct 2023

HAL is a multi-disciplinary open access archive for the deposit and dissemination of scientific research documents, whether they are published or not. The documents may come from teaching and research institutions in France or abroad, or from public or private research centers.

L'archive ouverte pluridisciplinaire **HAL**, est destinée au dépôt et à la diffusion de documents scientifiques de niveau recherche, publiés ou non, émanant des établissements d'enseignement et de recherche français ou étrangers, des laboratoires publics ou privés.

System identification of MISO fractional systems: parameter and differentiation order estimation

Stéphane Victor [a] Abir Mayoufi [a,b] Rachid Malti [a] Manel Chetoui [b] Mohamed Aoun [b]

[a] *Univ. Bordeaux, CNRS, IMS UMR 5218 – 351 cours de la Libération, 33405 Talence cedex, France*
firstname.lastname@ims-bordeaux.fr

[b] *University of Gabes, ENIG, MACS LR16ES22 – Avenue Omar Ibn El Khattab, Zrig, 6029 Gabes, Tunisia*
firstname.lastname@enig.rnu.tn

Abstract

This paper deals with continuous-time system identification of multiple-input single-output (MISO) fractional differentiation models. When differentiation orders are assumed to be known, coefficients are estimated using the simplified refined instrumental variable method for continuous-time fractional models extended to the MISO case. For unknown differentiation orders, a two-stage optimization algorithm is proposed with the developed instrumental variable for coefficient estimation and a gradient-based algorithm for differentiation order estimation. A new definition of structured-commensurability (or S-commensurability) is introduced to better cope with differentiation order estimation. Three variants of the algorithm are then proposed: (i) first, all differentiation orders are set as integer multiples of a global S-commensurate order, (ii) then, the differentiation orders are set as integer multiples of a local S-commensurate orders (one S-commensurate order for each subsystem), (iii) finally, all differentiation orders are estimated by releasing the S-commensurability constraint. The first variant has the smallest number of parameters and is used as a good initial hit for the second variant which in turn is used as a good initial hit for the third variant. Such a progressive increase of the number of parameters allows better performance of the optimization algorithm evaluated by Monte Carlo simulation analysis.

Key words: system identification, continuous-time, instrumental variable, multiple-input single-output (MISO) system, order optimization, fractional model

1 Introduction

Applications of fractional order systems (FOS) are numerous and closely linked to recursive and fractal geometry, for modeling: a porous dyke [30,31], thermal diffusive phenomena [7,22], charge diffusion in lithium-ion batteries [29,47], modeling Foucault currents inside rotor bars in induction machines [2], or even in biological systems [14,23,44].

System identification aims at providing a mathematical model for dynamical systems using a set of input and output data. Even though most system identification algorithms are developed in discrete time (DT), dynamical systems are generally expressed in continuous time (CT) to better describe physical systems governed by differential equations. New challenges appear on system identification as technology and society evolve: [46] provides new paradigms and challenges in system identification such as broader types of uncertainties, networked systems or even data explosion; [34] proposes kernel methods; [20] gives new kernel-based regularization methods; [3] proposes to estimate time-delay with sampled limit cycle in frequency domain; etc.

Instrumental Variable (IV) has been explored for several decades [48,37] in the discrete-time (DT) and was extended to the continuous-time in [52,50], as the refined instrumental variable (rivc) in presence of colored noise or as the Simplified rivc in presence of white noise [49]. When the model lies in the same class as the true system, the rivc method can be interpreted in optimal statistical terms as yielding consistent estimates with minimum variance. Both rivc and srivc methods use an iterative adaptive prefiltering based on a quasi-optimal statistical solution. Some developments aimed at extending the rivc method to handle multi-input models [10], hybrid Box–Jenkins models [11], irregularly sampled data [45], linear parameter varying models [17], CT output-error models with time-delay from relay feedback tests [3] and benchmark problems for continuous-time model identification [33]. A consistency analysis of the srivc method

for CT systems has been discussed recently in [32].

System identification with fractional order models (FOM) has become more and more important in different fields. First works started in the late nineties as pointed out in the state of the art in [24]. Since then, many other developments have been carried out, such as low order model identification of fractional systems [6], subspace method for state-space identification [41], multivariable non commensurate fractional systems [25], FOM with time delays [28], CT FOM in errors-in-variables context [4], parameter identification in fractional differential equations [15], inversion mechanism of functional extrema model via the differential evolution algorithms [8], identification of FOM using block pulse functions [40], system identification with measurement noise compensation based on polynomial modulating function [9], recursive identification method for fractional time-delay systems using a DT model [13], FOM identification using enhanced response sensitivity approach [18].

Initialization of fractional-order systems have been widely studied in the literature. Lorenzo and Hartley [21] have proposed to derive the Laplace transform for the initialized fractional integral and derivative of the Riemann-Liouville fractional calculus. Trigeassou and Maamri [42] have proposed an equivalence principle between the fractional system and an exactly equivalent infinite dimensional differential equation by using the fractional integration operator and the frequency distributed state space model. In fact, both methods are proven to be equivalent in a couple of examples in [12]. When system identification with non zero initial conditions is addressed, then the fractional system should be simulated by considering the initial conditions, with either of the two previous approaches, so that the time-response takes properly into account the initialization effect.

For coefficient estimation, the authors in [5] use state variable filters to cut noise in high frequencies so that the estimation variance can be reduced. Moreover, they also use instrumental variable technique (ivsvf) to obtain unbiased estimation. The Simplified Refined Instrumental Variable (sriv) approach was extended to fractional models in [43] where estimates are consistent with minimum variance.

In system identification with rational models, where only coefficients are estimated, the model order remains unchanged. When dealing with differentiation order estimation for fractional models, estimating both coefficients and differentiation orders is not a trivial task: indeed, the model order constantly varies at each iteration. As a consequence, a new definition of commensurability is introduced in this paper to avoid the explosion of parameter number. This Structured-commensurability definition is linked with the model structure and fixes the number of parameters. Then, the srivc algorithm is extended to multiple-input single-output fractional models (as the MISO-srivcf) for linear coefficient estimation, by assuming that all differentiation orders are known. Then, the paper proposes a gradient-based approach for differentiation order estimation which combines simultaneously the estimation of the coefficients and the differentiation orders. Three variants are proposed: first, all differentiation orders are set as integer multiples of a global S-commensurate order which is estimated; then, different local S-commensurate orders are estimated, one for each input-output model; and finally, the commensurability constraint is released and all differentiation orders are further independently optimized.

The paper is organized as follows. After recalling the fractional calculus and formulating the system identification problem in section 2, section 3 presents the srivcf algorithm extended to MISO systems for the coefficient estimation. Then, section 4 develops the differentiation order estimation with the proposed three variants. Finally, a conclusion is drawn in section 5.

2 MISO system context

2.1 Description of MISO fractional order systems

Consider a MISO fractional order system as illustrated in Fig.1 and described by the following relations:

$$\mathcal{S}: \begin{cases} y_k(t) = G_k(p)u_k(t) \\ y(t) = \sum\limits_{k=1}^{K} y_k(t) \\ y^*(t_h) = y(t_h) + e(t_h) \end{cases} \tag{1}$$

where $K \in \mathbb{N}$ is the number of inputs, and consequently the number of subsystems. Let $u(t) = [u_1(t), \ldots, u_K(t)]$ be the vector of uncorrelated input signals and p the differential operator ($p = \frac{d}{dt}$). The input-output data $(u(t), y(t))$ are collected at regular samples and assumed large enough to guarantee convergence of the estimated parameters to the true ones. The quasi-stationary input signals $\{u_k(t),\, 0 \leq t \leq t_{final}, k = 1, \ldots, K\}$ applied to the MISO system are persistently exciting and give rise to the output signal $\{y(t),\, 0 \leq t \leq t_{final}\}$. The output measurement $y(t)$ is corrupted by a discrete-time white noise $e(t_h)$ and G_k is the fractional operator that relates the input signal $u_k(t)$ to its noise-free output $y_k(t)$:

$$G_k(p,\theta) = \frac{B_k(p,\theta)}{A_k(p,\theta)} = \frac{\sum\limits_{j=0}^{M_k} b_{j,k} p^{\beta_{j,k}}}{1 + \sum\limits_{i=1}^{N_k} a_{i,k} p^{\alpha_{i,k}}} \tag{2}$$

where θ is the parameter vector defined in (13) and the differentiation orders are ordered positive real numbers

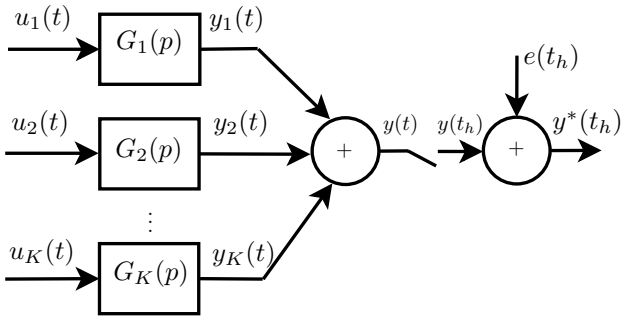

Fig. 1. MISO model structure

for identifiability purpose:

$$\begin{cases} 0 < \alpha_{1,k} < \alpha_{2,k} < ... < \alpha_{N_k,k} \\ 0 < \beta_{0,k} < \beta_{1,k} < ... < \beta_{M_k,k} \end{cases} \forall k = 1, \ldots, K.$$

It is assumed that $G_k(p)$ operators are strictly proper with $\alpha_{N_k,k} > \beta_{M_k,k}$, $\forall k$, that B_k and A_k are coprime polynomials, and that all the transfer functions $G_k(p)$ are asymptotically stable [26] .

Definition 2.1 (S-commensurability) *A SISO system G_1, for* a given model structure [1] (2)*, characterized by the number of terms M_1 and N_1, has a* structured-commensurate *(or S-commensurate) order*

$$\nu = \alpha_{1,1}, \tag{3}$$

if all its differentiation orders are successive integer multiples of ν, namely:

$$G_1(p) = \frac{\sum_{j=0}^{M_1} b_{j,1} p^{j\nu}}{1 + \sum_{i=1}^{N_1} a_{i,1} p^{i\nu}}. \tag{4}$$

For example, consider the following transfer function:

$$G_1(s) = \frac{1}{1 + 1.5s^{1.2} + 0.5s^{2.8}}.$$

According to the classic definition of commensurability (see [26]), G_1 is commensurate of order 0.4, namely:

$$G_1(s) = \frac{1}{1 + 1.5s^{3\times 0.4} + 0.5s^{7\times 0.4}}$$

[1] In the classic case [26], the definition of a commensurate system of order ν is independent of the model structure and may generate high order transfer function in s^ν. The proposed S-commensurability definition is linked to the model structure and therefore fixes the number of parameters to a prescribed value.

and generates a model order equal to 7 in $s^{0.4}$.

According to the new definition 2.1, G_1 is not S-commensurate, because the differentiation orders are not successive integer multiples of $\alpha_{1,1} = 1.2$.

2.2 Fractional calculus

The differentiation to an arbitrary order $\nu \in \mathbb{R}^+$ of a function $f(t)$, in the sense of Grünwald-Letnikov, is defined by:

$$p^\nu f(t) = \lim_{\ell \to 0} \frac{1}{\ell^\nu} \sum_{h=0}^{\lfloor \frac{t}{\ell} \rfloor} (-1)^h \binom{\nu}{h} f(t - h\ell) \tag{5}$$

where $\lfloor . \rfloor$ is the floor operator and $\binom{\nu}{h}$ is the Newton's binomial generalized to fractional orders as follows:

$$\binom{\nu}{h} = \frac{\Gamma(\nu+1)}{\Gamma(h+1)\Gamma(\nu-h+1)} = \frac{\nu(\nu-1)...(\nu-h+1)}{h!}.$$

Consequently, the fractional derivative of a function has a global characterization as the whole past of the function is required.

For $\nu = 1$, all binomials $\binom{\nu}{h} = 0$ when $h - \nu \in \mathbb{N}$, thus leading equation (5) to the classic definition of integer order derivative:

$$pf(t) = \lim_{\ell \to 0} \frac{f(t) - f(t-\ell)}{\ell}. \tag{6}$$

For numerical evaluation of the ν-th fractional derivative, parameter ℓ in (5) is replaced by a sampling period T and the limit is dropped:

$$p^\nu f(t) = \frac{1}{T^\nu} \sum_{h=0}^{\lfloor \frac{t}{T} \rfloor} (-1)^h \binom{\nu}{h} f(t - Th) + \mathcal{O}(T). \tag{7}$$

So defined, as stated in [35, section 7.4], the error terms are proportional to the sampling period. Therefore, to make the approximation error negligible, the sampling time must be sufficiently small [2] .

[2] Note that a too small sampling period may also provide numerical issues such as stability in digital implementation. In this case, suitable discrete rational approximations might be preferred.

Time-domain simulation of fractional systems being a thoroughly studied topic in the literature, system identification algorithms proposed in this paper are meant to be independent from time-domain simulation algorithms. Nevertheless, FOMs should be correctly simulated with negligible simulation errors for the parameter estimation to be consistent.

The Laplace transform of the ν-th derivative of a causal function f ($f(t) = 0 \forall t \leq 0$), is given by [35, section 2.8.4]:

$$\mathscr{L}\{p^\nu x(t)\} = s^\nu X(s), \tag{8}$$

s denoting the Laplace variable. This result proves to be also in accordance with the classic rational case when ν is an integer.

Definition 2.2 (Local S-commensurability) *A MISO system, for a given model structure* (2)*, has* local S-commensurate orders ν_k *if each subsystem* G_k *has its own S-commensurate order (see Definition 2.1)*

$$\nu_k = \alpha_{1,k} \quad \textit{for} \quad k = 1, \ldots, K.$$

Therefore, each transfer function can be rewritten as:

$$G_k(p) = \frac{\sum_{j=0}^{M_k} b_{j,k} p^{j\nu_k}}{1 + \sum_{i=1}^{N_k} a_{i,k} p^{i\nu_k}}. \tag{9}$$

Definition 2.3 (Global S-commensurability) *A MISO system, for a given model structure* (2)*, has a* global S-commensurate order ν *if all its subsystems have the same S-commensurate order according to Definition 2.2 :*

$$\nu = \alpha_{1,1} = \alpha_{1,2} = \cdots = \alpha_{1,K},$$

Therefore, each transfer function can be rewritten as:

$$G_k(p) = \frac{\sum_{j=0}^{M_k} b_{j,k} p^{j\nu}}{1 + \sum_{i=1}^{N_k} a_{i,k} p^{i\nu}}. \tag{10}$$

For an S-commensurate FOS, the most used stability theorem is the one proposed by Matignon [26] extended to commensurate orders between 1 and 2.

Theorem 2.1 (Stability theorem, SISO case) *Let* G_1 *be a SISO S-commensurate transfer function and* ν *its S-commensurate order.* $G_1(s) = \frac{Q_\nu(s)}{P_\nu(s)}$ *is stable, in the bounded input bounded output sense, if and only if:*

$$0 < \nu < 2 \tag{11}$$

and

$$\forall s_k \in \mathbb{C}, P_\nu(s_k) = 0 \quad \textit{such as} \quad |\arg(s_k)| > \nu\frac{\pi}{2}. \tag{12}$$

□

As in the rational case, if all subsystems are stable then the MISO fractional system is stable too.

2.3 Problem formulation

The objective is to estimate the parameters of the MISO model $\mathcal{S}$ described by equation (1) by using H samples of input/output data $\{u_1(t_h), ..., u_K(t_h), y^*(t_h)\}_{h=1}^H$, between $t_1 = 0$ and $t_H = t_{final}$.

The parameter vector, θ, is defined as

$$\theta = \begin{bmatrix} \rho \\ \mu \end{bmatrix} \tag{13}$$

- where ρ gathers all the MISO transfer function coefficients
$$\rho = \left[\rho_1^T, \ \ldots, \ \rho_K^T\right]^T \tag{14}$$
with
$$\rho_k^T = [b_{0,k}, b_{1,k}, \ldots, b_{M_k,k}, a_{1,k}, \ldots, a_{N_k,k}]$$
for $k = 1, \ldots, K$; hence, ρ has a total number of coefficients of $\sum_{k=1}^K (N_k + M_k + 1)$
- and where μ gathers all the MISO transfer function differentiation orders, that can be defined according to the following cases,

Case 1: if a global S-commensurate order is sought, then the differentiation order vector is reduced to a single parameter

$$\mu = \nu; \tag{15}$$

Case 2: if local S-commensurate orders are sought, then the differentiation order vector is extended to K parameters

$$\mu = \left[\nu_1, \ \ldots, \ \nu_K\right]^T; \tag{16}$$

Case 3: if the MISO model is non commensurate, then μ gathers all the differentiation orders

$$\mu = \left[\mu_1^T, \ \ldots, \ \mu_K^T\right]^T \tag{17}$$

with

$$\mu_k^T = \left[\beta_{0,k}, \beta_{1,k}, \ldots, \beta_{M_k,k}, \alpha_{1,k}, \ldots, \alpha_{N_k,k}\right]$$

for $k = 1, ..., K$; hence, μ has a total number of differentiation orders of $\sum_{k=1}^{K}(N_k + M_k + 1)$.

It is well known that the methods based on least squares give biased parameters in presence of noise affecting the output measurements. To solve this problem, methods based on instrumental variables are used.

3 Refined Instrumental Variable for Continuous-time fractional models

In this section, the true model structure is assumed known as well as all the fractional differentiation orders. Thus, only the linear coefficients of the MISO models are estimated. Hence, the unknown parameter vector θ is reduced to ρ.

3.1 Recall of the srivcf algorithm for SISO models [43]

The srivcf approach was developed in [43] for SISO system identification by fractional models and is based on turning maximum likelihood estimation on a pseudo-linear form that involves optimal prefilters.

Consider a SISO fractional system, as defined in (1) (with $K = 1$), corrupted by a white additive measurement noise. The unknown parameter vector θ is reduced to $\theta_1 = \rho_1$, and consequently, only dependencies on ρ_1 are highlighted in the following equations.

According to the prediction error method, a suitable error function ε_1 can be defined as an output error:

$$\varepsilon_1(t,\theta) = y^*(t) - \frac{B_1(p,\theta)}{A_1(p,\theta)}u(t), \tag{18}$$

or even,

$$\begin{aligned}\varepsilon_1(t,\theta) =& A_1(p,\theta)\left(\frac{1}{A_1(p,\theta)}y^*(t)\right)\\ &- B_1(p,\theta)\left(\frac{1}{A_1(p,\theta)}u(t)\right).\end{aligned} \tag{19}$$

This expression well shows that the optimal prefilter, to be applied on both input and output signals, is

$$F_1^{opt}(p) = \frac{1}{A_1(p,\theta)}, \tag{20}$$

a transfer function which cannot be obtained in practice, as θ and consequently $A_1(p,\theta)$ are unknown. To solve this problem, an iterative procedure is usually implemented, to iteratively adjust the estimates until convergence. Hence, the following filter is initialized and computed iteratively:

$$F^{\text{iter}}(p) = \frac{1}{\hat{A}_1(p,\hat{\theta}^{iter})} = \frac{1}{1 + \sum\limits_{i=1}^{N} \hat{a}_{i,1}p^{\alpha_{i,1}}}, \tag{21}$$

where iter $= 1, 2, \ldots$ denotes the iteration number, and $\hat{a}_{i,1}$ is the coefficient estimated at iter. The detailed algorithm can be found in [43].

Moreover, it is shown in [43], when the quasi-stationary input signal is persistently exciting and the noise signal is white with zero mean, that the srivcf algorithm is asymptotically unbiased thanks to the IV mechanism.

3.2 srivcf algorithm for MISO models

One of the contributions of this paper is to propose an extension of the SISO srivc method to fractional MISO models described by (1). It can also be considered as a generalized extension of rational MISO system case, as developed in [10], to fractional MISO models.

The basic idea is to estimate the coefficients vector ρ_k, for each subsystem G_k, $k = 1, \ldots, K$, while assuming that all the other coefficients ρ_n (with $n \neq k$) are known, by applying the SISO version of the srivcf algorithm, as proposed in section 3.1.

As a consequence, a suitable error function ε_k, associated with the submodel G_k, is defined as follows:

$$\varepsilon_k(t,\theta) = x_k(t,\theta) - y_k(t,\theta), \quad k = 1, ..., K \tag{22}$$

where y_k is the noise-free part of x_k:

$$x_k(t,\theta) = y^*(t) - \sum_{\substack{n=1\\ n\neq k}}^{K} y_n(t,\theta). \tag{23}$$

Relation (22) can be rewritten as:

$$\begin{aligned}\varepsilon_k(t,\theta) =& A_k(p,\theta)\left(\frac{1}{A_k(p,\theta)}x_k(t,\theta)\right)\\ &- B_k(p,\theta)\left(\frac{1}{A_k(p,\theta)}u_k(t)\right),\end{aligned} \tag{24}$$

which well shows that the optimal prefilter, to be applied on both input and output signals, is

$$F_{opt,k}(p) = \frac{1}{A_k(p,\theta)}, \tag{25}$$

a transfer function which cannot be obtained in practice, as θ and consequently $A_k(p,\theta)$ are unknown.

To solve this problem, again, an iterative procedure is applied, which is intended to iteratively adjust the estimates until convergence. Hence, the following filter is initialized and computed iteratively:

$$F_k^{\text{iter}}(p) = \frac{1}{\hat{A}_k(p, \hat{\theta}^{\text{iter}})} = \frac{1}{1 + \sum_{i=1}^{N_k} \hat{a}_{i,k} p^{\alpha_{i,k}}}, \tag{26}$$

where iter $= 1, 2, \ldots$ denotes the iteration number, and $\hat{a}_{i,k}$ is the coefficient estimated at iter.

The MISO version of srivcf is described in algorithm 1.

Algorithm 1 *Summary of the MISO-srivcf algorithm for coefficient estimation*

Step 1: Initialization
iter $= 0$
Initialize the parameter vector $\theta^0 = \rho^0$
Step 2: Iterative IV estimation

for *each subsystem* $k = 1, \ldots, K$
do

i. iter $=$ *iter* $+ 1$
Update the auxiliary model with parameter vector $\hat{\theta}^{iter-1}$*:*

$$\hat{G}_k^{iter}(p, \hat{\theta}^{iter-1}) = \frac{\hat{B}_k^{iter}(p, \hat{\theta}^{iter-1})}{\hat{A}_k^{iter}(p, \hat{\theta}^{iter-1})}$$

and generate the instruments:

$$y_k(t, \hat{\theta}^{iter-1}) = \hat{G}_k^{iter}(p, \hat{\theta}^{iter-1}) u_k(t).$$

ii. Compute the response $x_k(t, \hat{\theta}_k^{iter-1})$ *to* $u_k(t)$*:*

$$x_k(t, \hat{\theta}^{iter-1}) = y^*(t) - \sum_{\substack{n=1 \\ n \neq k}}^{K} y_n(t, \hat{\theta}^{iter}).$$

iii. Update the prefilter:

$$F_k^{iter}(p) = \frac{1}{\hat{A}_k(p, \hat{\theta}^{iter-1})}.$$

iv. Evaluate the prefiltered derivatives:

$$\begin{cases} p^{\beta_{j,k}} u_{k,f}(t) = p^{\beta_{j,k}} F_k^{iter}(p) u_k(t) \\ p^{\alpha_{i,k}} y_{k,f}(t) = p^{\alpha_{i,k}} F_k^{iter}(p) y_k(t) \\ p^{\alpha_{i,k}} x_{k,f}(t) = p^{\alpha_{i,k}} F_k^{iter}(p) x_k(t). \end{cases}$$

v. Compute the new estimates

$$\hat{\rho}_k^{iter} = \left({\Phi_{k,f}^{iv}}^T \Phi_{k,f}^* \right)^{-1} {\Phi_{k,f}^{iv}}^T X_{k,f}$$

where the instrumental matrix is

$$\Phi_{k,f}^{iv} = \left[\varphi_{k,f}^{iv}(t_1), ..., \varphi_{k,f}^{iv}(t_H) \right]^T$$

$$\varphi_{k,f}^{iv}(t) = \begin{bmatrix} p^{\beta_{0,k}} u_{k,f}(t) ... p^{\beta_{M_k,k}} u_{k,f}(t) \\ -p^{\alpha_{1,k}} y_{k,f}^{iter}(t) ... - p^{\alpha_{N_k,k}} y_{k,f}^{iter}(t) \end{bmatrix},$$

the regression matrix is

$$\Phi_{k,f}^* = \left[\varphi_{k,f}^*(t_1), ..., \varphi_{k,f}^*(t_H) \right]^T,$$

$$\varphi_{k,f}^*(t) = \begin{bmatrix} p^{\beta_{0,k}} u_{k,f}(t) ... p^{\beta_{M_k,k}} u_{k,f}(t) \\ -p^{\alpha_{1,k}} x_{k,f}^{iter}(t) ... - p^{\alpha_{N_k,k}} x_{k,f}^{iter}(t) \end{bmatrix}$$

and the filtered output vector is

$$X_{k,f} = \left[x_{k,f}(t_1), ..., x_{k,f}(t_H) \right]^T.$$

vi. Update the parameter vector

$$\hat{\theta}^{iter} = \left[\hat{\rho}_1^{iter}, \ldots, \hat{\rho}_k^{iter}, \ldots, \hat{\rho}_K^{iter} \right]^T.$$

while $\sum_{j=1}^{\dim \hat{\rho}_k} \left| \frac{\hat{\rho}_{k,j}^{iter} - \hat{\rho}_{k,j}^{iter-1}}{\hat{\rho}_{k,j}^{iter}} \right| > \epsilon_1$

where $\hat{\rho}_{k,j}^{iter}$ *corresponds to the* j*-th element of the parameter vector* $\hat{\rho}_k^{iter}$ *at iteration iter and* ϵ_1 *is a scalar that is set for a given precision of the estimates.*

Step 3: *Compute the parametric covariance matrix* P_ρ

$$P_\rho = \hat{\sigma}^2 \, diag \left(P_{\rho_1}, \ldots, P_{\rho_K} \right) \tag{27}$$

where, for $k = 1, ..., K$

$$P_{\rho_k} = \left({\Phi_{k,f}^{iv}}^T \Phi_{k,f}^{iv} \right)^{-1} \tag{28}$$

and $\hat{\sigma}^2$ *being the variance of the empirical estimation of the noise given by:*

$$y^*(t) - \sum_{k=1}^{K} y_k(t)$$

where $y_k(t)$ *is calculated at the last iteration.*

When the noise signal is normally distributed, the srivcf estimates can be interpreted in optimal statistical terms yielding consistent estimates with minimum variance, assessed by comparing the covariance matrix to the best possible accuracy given by the Cramér -Rao lower bound (CRB) [16,39,51]. Thus, the CRB can be computed as:

$$P_\rho^{CRB} = \frac{\sigma^2}{H} \text{diag} \left(P_{\rho_1}^{CRB}, \ldots, P_{\rho_K}^{CRB} \right) \tag{29}$$

where σ^2 is the true noise variance and

$$P_{\rho_k}^{CRB} = \left(E\left[\varphi_{k,f}^{iv,opt}(t_h)^T \varphi_{k,f}^{iv,opt}(t_h)\right]\right)^{-1} \tag{30}$$

are obtained with the optimally noise-free pre-filtered IV vector:

$$\varphi_{k,f}^{iv,opt}(t_h) = F_k^{opt}(p)\begin{bmatrix} p^{\beta_{0,k}}u_k(t_h)\dots p^{\beta_{M_k,k}}u_k(t_h) \\ -p^{\alpha_{1,k}}y_k(t_h)\dots - p^{\alpha_{N_k,k}}y_k(t_h)\end{bmatrix}^T, \tag{31}$$

filtered with the optimal filter:

$$F_k^{opt}(p) = \frac{1}{A_k(p,\theta)}. \tag{32}$$

3.3 *Simulation example 1 — identification of a global S-commensurate system*

Consider a simulation example where the data are generated from the MISO system:

$$S_1 : \begin{cases} y_1(t) = \frac{1}{3p^{0.25}+1}u_1(t), \\ y_2(t) = \frac{2}{2p^{0.5}+1}u_2(t), \\ y_3(t) = \frac{5}{p^{0.75}+1}u_3(t), \\ y(t) = \sum_{k=1}^{3} y_k(t) \\ y^*(t_h) = y(t_h) + e(t_h). \end{cases} \tag{33}$$

Three uncorrelated pseudo random binary sequences (prbs), u_i for $i = 1, 2, 3$, are applied to (33). The inputs are persistent and excite the subsystems in an appropriate frequency band. The length of each prbs is set to $3 \times \tau_{max}$, where $\tau_{max} = \max(3^{1/0.25}, 2^{1/0.5}, 1^{1/0.75})$. The sum of the three output responses provides the noise-free output $y(t)$, which is corrupted by a zero mean Gaussian white noise, with a noise to signal ratio (NSR) set to -20dB, to produce the output measurement $y^*(t)$ (see Fig. 2). In this simulation, the sampling period is set to $T = 0.05s$.

All simulations have been carried out with the CRONE toolbox developed in Matlab® , which is dedicated to fractional calculus, fractional system simulation and system identification with fractional models [3] .

[3] The new version of the CRONE toolbox is an object-oriented version with several classes defined for fractional models (LTI, explicit form, implicit form, ZPK, state-space representation, etc.). This CRONE toolbox is freely available at http://archive.ims-bordeaux.fr/CRONE/toolbox/

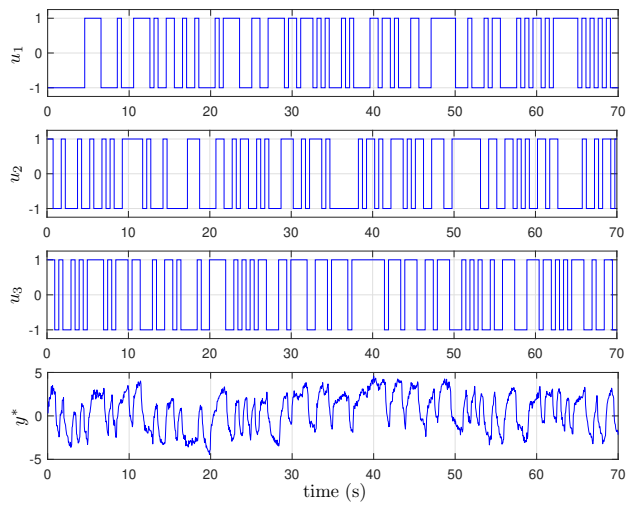

Fig. 2. Input/output data used for the identification of system (33)

3.3.1 *Coefficient estimation with known differentiation orders*

Assume that the true model structure is described for each subsystem $k = 1, \dots, 3$ by:

$$G_k(t) = \frac{b_{0,k}}{1 + a_{1,k}p^{\alpha_{1,k}}}, \tag{34}$$

and that the differentiation orders are known as in (33). The objective is to estimate the coefficients of all the subsystems and to check the efficacy of the algorithm through a Monte Carlo analysis, with 75 runs.

Table 1 illustrates the synthesis of the Monte Carlo simulation and the performances of the MISO srivcf method. Thanks to the IV mechanism, the MISO srivcf algorithm provides consistent unbiased estimates and low variance, this latter being confirmed by comparing the Euclidean norms of the covariance matrix and the CRB:

$$\|P_\rho\|_2 = 2.107\,10^{-3} \geq \left\|P_\rho^{CRB}\right\|_2 = 1.619\,10^{-3}.$$

3.3.2 *Coefficient estimation with unknown differentiation orders*

In practice, the differentiation orders are not always known *a priori*. Let us now evaluate the influence of a global S-commensurate order estimation by computing the cost function, defined as the ℓ_2-norm of the normalized output error:

$$J_{\text{dB}}(\hat{\theta}) = 10\log\frac{||\varepsilon(t,\hat{\theta})||_2^2}{||\hat{y}(t)||_2^2} \tag{35}$$

Table 1
Monte Carlo simulation of 75 runs for coefficient estimation with the MISO srivcf ($\bar{\rho}$ is the mean and $\hat{\sigma}_\rho$ the standard deviation)

	True	srivcf	
	ρ	$\bar{\rho}$	$\hat{\sigma}_\rho$
$b_{0,1}$	1	1.0096	0.0919
$a_{1,1}$	3	3.0161	0.3623
$b_{0,2}$	2	1.9996	0.0349
$a_{1,2}$	2	1.9983	0.0481
$b_{0,3}$	5	5.0017	0.0122
$a_{1,3}$	1	1.0009	0.0046

where the output error $\varepsilon(t,\hat{\theta})$ is defined as:

$$\varepsilon(t,\hat{\theta}) = y^*(t) - \hat{y}(t,\hat{\theta}) \tag{36}$$

and the estimated output $\hat{y}(t,\hat{\theta})$ is defined as:

$$\hat{y}(t) = \sum_{k=1}^{K} y_k(t). \tag{37}$$

Varying the global S-commensurate order, between $\nu = 0.35$ and $\nu = 1.35$, and applying the srivcf method on the MISO system (33), the cost function J, defined in (35), is computed for different global S-commensurate orders and plotted in Fig. 3.

If all submodels were in the same model class as the true subsystems, the minimum of the cost function would have equalled the NSR $= -20dB$. Here, the minimum of the cost function is found at $\nu = 0.75$ and equals -19dB. Consequently, the modeling error is approximately equal to 1dB. For $\nu = 0.6$ the cost function is around -16dB, with a modeling error around 4dB.

This simulation result motivates estimating the fractional differentiation orders, as they may considerably influence the results.

4 Differentiation order estimation

4.1 Two-stage algorithm for coefficient and differentiation order estimations

In the case when the differentiation orders are unknown, it is helpful to consider order estimation along with the transfer function coefficients. A two stage algorithm is proposed to identify all the parameters (coefficients and differentiation orders): the srivcf MISO algorithm is used for coefficient estimation and a gradient-based algorithm is used for differentiation order optimization.

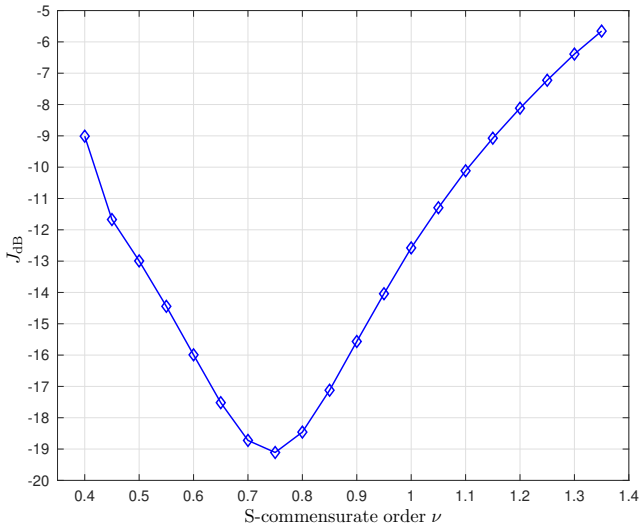

Fig. 3. Cost function versus the global S-commensurate order in example 1

Two-stage algorithms have been used in the literature in different contexts (see. *e.g.* [1,27,36,38,43]). Although they do not have a proof of convergence, it has been noted in these references that they do often converge to a minimum. Moreover, the latter reference has successfully estimated the parameters with the same strategy applied to SISO systems. Three variants of order optimization algorithm are proposed: the first variant has the smallest number of parameters and is used as a good initial hit for the second variant which in turn is used as a good initial hit for the third variant which is the most general case.

4.2 Differentiation order estimation

The estimation problem is formulated as a minimization problem of the ℓ_2-norm:

$$J(\hat{\theta}) = \frac{1}{2}\left\|\varepsilon(t,\hat{\theta})\right\|_2^2 = \frac{1}{2}\mathrm{E}^T\mathrm{E}, \tag{38}$$

where

$$\mathrm{E} = \left[\varepsilon(t_1,\hat{\theta}),\ldots,\varepsilon(t_H,\hat{\theta})\right]^T,$$

contains the output error $\varepsilon(t,\hat{\theta})$ defined in (36) for all the instants.

A Gauss–Newton algorithm (see [19, chap. 10]) is used for the estimation of the differentiation orders. This algorithm allows to iteratively compute the differentiation order vector μ^{iter}:

$$\mu^{\mathrm{iter}} = \mu^{\mathrm{iter}-1} - \lambda\left[\mathscr{H}^{-1}\frac{\partial J}{\partial \mu}\right] \tag{39}$$

where λ is a weighting factor, $\frac{\partial J}{\partial \mu}$ is the gradient defined as

$$\frac{\partial J}{\partial \mu} = \Upsilon^T\mathrm{E}, \tag{40}$$

where

$$\Upsilon^T = \left[\frac{\partial\varepsilon}{\partial\mu}(t_1,\hat{\theta}),\ldots,\frac{\partial\varepsilon}{\partial\mu}(t_H,\hat{\theta})\right] \tag{41}$$

and $\mathscr{H}$ is the approximated Hessian given by

$$\mathscr{H} = \Upsilon^T\Upsilon. \tag{42}$$

The differentiation order μ is set to any vector: (15), (16) or (17), according to whether the global S-commensurate order is estimated, the local ones, or all the orders. The error sensitivity function $\frac{\partial\varepsilon(t,\hat{\theta})}{\partial\mu}$ is computed accordingly.

Case 1: If μ is defined as a global S-commensurate order ν for all subsystems such as in (15), then

$$\frac{\partial\varepsilon}{\partial\mu} = \frac{\partial\varepsilon}{\partial\nu} = -\sum_{k=1}^{K}\frac{\partial\hat{y}_k}{\partial\nu}. \tag{43}$$

where the output sensitivity functions are given, for $k = 1,\ldots,K$:

$$\frac{\partial\hat{y}_k}{\partial\nu} = \left[\sum_{j=0}^{M_k} j\hat{b}_{j,k}p^{j\nu} + \sum_{j=0}^{M_k}\sum_{i=1}^{N_k}(j-i)\hat{b}_{j,k}\hat{a}_{i,k}p^{(i+j)\nu}\right] \times \frac{\ln(p)}{\left(1+\sum\limits_{i=1}^{N_k}\hat{a}_{i,k}p^{i\nu}\right)^2}u_k(t). \tag{44}$$

Case 2: If μ is defined as the vector of local S-commensurate orders ν_k, as in (16), then

$$\frac{\partial\varepsilon}{\partial\mu} = \left[\frac{\partial\varepsilon}{\partial\nu_1},\ldots,\frac{\partial\varepsilon}{\partial\nu_K}\right] = \left[-\frac{\partial\hat{y}_1}{\partial\nu_1},\ldots,-\frac{\partial\hat{y}_K}{\partial\nu_K}\right]. \tag{45}$$

where the output sensitivity functions are given for $k = 1,\ldots,K$:

$$\frac{\partial\hat{y}_k}{\partial\nu_k} = \left[\sum_{j=0}^{M_k} j\hat{b}_{j,k}p^{j\nu_k} + \sum_{j=0}^{M_k}\sum_{i=1}^{N_k}(j-i)\hat{b}_{j,k}\hat{a}_{i,k}p^{(i+j)\nu_k}\right] \times \frac{\ln(p)}{\left(1+\sum\limits_{i=1}^{N_k}\hat{a}_{i,k}p^{i\nu_k}\right)^2}u_k(t). \tag{46}$$

Case 3: If μ is the vector of all the differentiation orders, as in (17), then

$$\frac{\partial\varepsilon}{\partial\mu} = \left[\frac{\partial\varepsilon}{\partial\mu_1^T},\ldots,\frac{\partial\varepsilon}{\partial\mu_K^T}\right]^T, \tag{47}$$

$$\frac{\partial\varepsilon}{\partial\mu_k^T} = \left[-\frac{\partial\hat{y}_k}{\beta_{0,k}},\ldots,-\frac{\partial\hat{y}_k}{\partial\beta_{M_k,k}},-\frac{\partial\hat{y}_k}{\partial\alpha_{1,k}},\ldots,-\frac{\partial\hat{y}_k}{\partial\alpha_{N_k,k}}\right] \tag{48}$$

with $k = 1,\ldots,K$ and the output sensitivity functions are given by:

$$\begin{aligned}\frac{\partial\hat{y}_k}{\partial\beta_{j,k}} &= \frac{\ln(p)\hat{b}_{j,k}p^{\hat{\beta}_{j,k}}}{1+\sum\limits_{i=1}^{N_k}\hat{a}_{i,k}p^{\hat{\alpha}_{i,k}}}u_k(t)\\ \frac{\partial\hat{y}_k}{\partial\alpha_{\ell,k}} &= \frac{\ln(p)\hat{a}_{\ell,k}p^{\hat{\alpha}_{\ell,k}}\sum\limits_{j=0}^{M_k}\hat{b}_{j,k}p^{\hat{\beta}_{j,k}}}{\left(1+\sum\limits_{i=1}^{N_k}\hat{a}_{i,k}p^{\hat{\alpha}_{i,k}}\right)^2}u_k(t),\end{aligned} \tag{49}$$

for $j = 0,\ldots,M_k$, $\ell = 1,\ldots,N_k$.

4.3 ***Summary of the MISO-oosrivcf algorithm***

The MISO-oosrivcf main steps are summarized in algorithm 2 where the differentiation order vector μ is estimated along with the coefficients.

Algorithm 2 *Summary of MISO-oosrivcf algorithm for all parameter estimation*

Step 1: Initialization
iter $= 0$
Initialize $\hat{\mu}^0$ *and compute* $\hat{\rho}^0$ *with the srivcf method.*
With $\hat{\theta}^0 = \begin{bmatrix}\hat{\rho}^0\\ \hat{\mu}^0\end{bmatrix}$, *compute the cost function* $J(\hat{\theta}^0)$ *from* (38).

Step 2: Iterative all parameter estimation
do
i. *iter* $=$ *iter* $+1$
ii. Coefficient estimation
Compute the coefficient vector $\hat{\rho}^{iter}$ *with MISO-srivcf (see algorithm 1)*
iii. Differentiation order estimation
Initialize $\lambda = \Lambda$ *(usually to 1)*
do

a. *Evaluate the cost function* $J\left(\begin{bmatrix}\hat{\rho}^{iter}\\ \hat{\mu}^{iter-1}\end{bmatrix}\right)$ *from* (38)

b. *Refine the order estimate* $\hat{\mu}^{iter}$*:*

$$\hat{\mu}^{iter} = \hat{\mu}^{iter-1} - \lambda\left[\mathscr{H}^{-1}\frac{\partial J}{\partial\mu}\right]_{\mu=\hat{\mu}^{iter-1}} \tag{50}$$

c. *Evaluate* $J\left(\begin{bmatrix}\hat{\rho}^{iter}\\ \hat{\mu}^{iter}\end{bmatrix}\right)$ *from* (38)

d. Set $\lambda = \frac{\lambda}{2}$

while $J\left(\begin{bmatrix}\hat{\rho}^{iter}\\ \hat{\mu}^{iter}\end{bmatrix}\right) > J\left(\begin{bmatrix}\hat{\rho}^{iter}\\ \hat{\mu}^{iter-1}\end{bmatrix}\right)$

iv. Form the parameter vector $\hat{\theta}^{iter}$*:*

$$\hat{\theta}^{iter} = \begin{bmatrix}\hat{\rho}^{iter}\\ \hat{\mu}^{iter}\end{bmatrix}$$

while $\sum_{\ell=1}^{\dim \hat{\rho}_k} \left| \frac{\hat{\theta}_\ell^{iter} - \hat{\theta}_\ell^{iter-1}}{\hat{\theta}_\ell^{iter-1}} \right| > \epsilon_2$

where $\hat{\theta}_\ell^{iter}$ *corresponds to the* ℓ*-th element of the order vector* $\hat{\theta}^{iter}$ *at iteration iter*

Step 3: *Compute the parametric covariance matrix* P_θ*:*

$$P_\theta = \hat{\sigma}^2 \mathscr{H}^{-1}$$

with $\hat{\sigma}^2$ *being the variance of the empirical estimation of the noise given by:*

$$y^*(t) - \sum_{k=1}^{K} y_k(t)$$

where $y_k(t)$ *is calculated at the last iteration and the approximated Hessian* $\mathscr{H}$ *is given in* (42)*.*

Note that ϵ_1 in algorithm 1 and ϵ_2 in algorithm 2 are scalars that are set for a given precision of the estimates. After convergence of $\hat{\theta}$, the parametric covariance matrix can be computed by using the approximated Hessian, defined as in (42), where the appropriate Υ is now defined by

$$\Upsilon^T = \left[\frac{\partial \varepsilon}{\partial \theta}(t_1, \hat{\theta}), \ldots, \frac{\partial \varepsilon}{\partial \theta}(t_H, \hat{\theta})\right]. \quad (51)$$

The discretized sensitivity functions, $\frac{\partial \varepsilon(t,\hat{\theta})}{\partial \theta}$, with respect to all parameters in θ, are defined as

$$\frac{\partial \varepsilon(t,\hat{\theta})}{\partial \theta} = \begin{bmatrix}\frac{\partial \varepsilon(t,\hat{\theta})}{\partial \rho}\\ \frac{\partial \varepsilon(t,\hat{\theta})}{\partial \mu}\end{bmatrix} \quad (52)$$

where $\frac{\partial \varepsilon}{\partial \mu}$ is given according to whether the global S-commensurate order (43), the local S-commensurate orders (45) or all differentiation orders (47) are estimated and

$$\frac{\partial \varepsilon}{\partial \rho} = \left[\frac{\partial \varepsilon}{\partial \rho_1^T}, \ldots, \frac{\partial \varepsilon}{\partial \rho_K^T}\right]^T \quad (53)$$

where

$$\frac{\partial \varepsilon}{\partial \rho_k^T} = -\left[\frac{\partial \hat{y}_k}{\partial b_{0,k}}, \ldots, \frac{\partial \hat{y}_k}{\partial b_{M_k,k}}, \frac{\partial \hat{y}_k}{\partial a_{1,k}}, \ldots, \frac{\partial \hat{y}_k}{\partial a_{N_k,k}}\right]. \quad (54)$$

Here $\frac{\partial \hat{y}_k}{\partial b_{j,k}}$ and $\frac{\partial \hat{y}_k}{\partial a_{i,k}}$ are the output sensitivity functions, given by:

$$\frac{\partial \hat{y}_k}{\partial b_{j,k}} = \frac{p^{\hat{\beta}_{j,k}}}{1 + \sum_{i=1}^{N_k} \hat{a}_{i,k} p^{\hat{\alpha}_{i,k}}} u_k(t), \quad \forall j = 0, \ldots, M_k, \quad (55)$$

$$\frac{\partial \hat{y}_k}{\partial a_{i,k}} = \frac{-\sum_{j=0}^{M_k} \hat{b}_{j,k} p^{\hat{\beta}_{j,k} + \hat{\alpha}_{i,k}}}{\left(1 + \sum_{i=1}^{N_k} \hat{a}_{i,k} p^{\hat{\alpha}_{i,k}}\right)^2} u_k(t), \ \forall i = 1, \ldots, N_k \quad (56)$$

with $k = 1, \ldots, K$.

4.4 Simulation examples

In this section, two examples are treated to illustrate the convergence and the efficacy of the proposed MISO-oosrivcf algorithm. In the first example, the system is described with local S-commensurate order subsystems. First, a global S-commensurate order is estimated which is then used for initializing the following stage: local S-commensurate order estimation. In the second example, the commensurability constraint is released so that all differentiation orders of each subsystem are estimated: first, a global S-commensurate order is estimated for all subsystems which is used for initializing the following stage with local S-commensurate orders which in turn initializes the final stage for the estimation of all differentiation orders.

4.4.1 Example 2 — S-commensurate order estimation combined with the srivcf algorithm

The data generating system (33) is used as described in section 3.3. The model structure is set as the true one (34):

$$\nu = \alpha_{1,1} = \alpha_{1,2} = \alpha_{1,3}. \quad (57)$$

When estimating a global S-commensurate order and after initializing it to $\nu = 1.1$, the MISO-oosrivcf algorithm converges to:

$$\hat{S} : \begin{cases} \hat{G}_1(s) = \dfrac{0.273}{0.2118 s^{0.751} + 1} \\ \hat{G}_2(s) = \dfrac{1.121}{0.760 s^{0.751} + 1} \\ \hat{G}_3(s) = \dfrac{4.878}{0.9676 s^{0.751} + 1}, \end{cases} \quad (58)$$

which is coherent with Fig. 3.

In this case, the cost function (35) is equal to -19.1dB. Recalling that the NSR equals -20dB, the ℓ_2-norm of the modeling error is evaluated to 0.9dB at the estimated global S-commensurate order model (58).

Table 2
Monte Carlo simulation with 75 runs for the estimation of local S-commensurate orders and coefficients ($\bar{\theta}$ is the mean and $\hat{\sigma}_\theta$ the standard deviation of the estimates)

	True	oosrivcf-MISO	
	θ	$\bar{\bar{\theta}}$	$\hat{\sigma}_\theta$
$b_{0,1}$	1	1.0053	0.0843
$a_{1,1}$	3	3.0138	0.2998
$\alpha_{1,1}$	0.25	0.2495	0.0122
$b_{0,2}$	2	2.0019	0.0459
$a_{1,2}$	2	2.0056	0.0655
$\alpha_{1,2}$	0.5	0.5006	0.0053
$b_{0,3}$	5	5.0180	0.0103
$a_{1,3}$	1	1.0062	0.0034
$\alpha_{1,3}$	0.75	0.7497	0.0012

Recall that the true system (33) is a local S-commensurate system according to definition 2.2. In this first variant, a global S-commensurate model is sought and the estimated model has converged to model (58). The submodels $\hat{G}_1$ and $\hat{G}_2$ have not converged to the true local S-commensurate models. Therefore they are not in the same class of the true submodels. Consequently, their corresponding estimated coefficients compensate the modeling errors linked to the differentiation orders. On the contrary, submodel $\hat{G}_3$ has converged to its true local S-commensurate order, probably due to its high gain, as compared to the static gains of G_1 and G_2. Consequently, its corresponding estimated coefficients have converged to the true ones (up to the noise effect).

For the second variant, the parameters of system (58) are used as initialization to evaluate local S-commensurate orders. A Monte Carlo simulation with 75 runs has been carried out with difrerent noise realizations and a NSR $= -20$dB. The results are provided in table 2, with a mean value close to the true local S-commensurate orders. The proposed MISO-oosrivcf algorithm for local S-commensurate orders and coefficient estimation is therefore validated as the estimated parameters have converged to the true ones with a very low variance.

Fig.4 well shows that, by using the system $\hat{S}$ defined in (58) as an initial hit, the MISO-oosrivcf algorithm converges to the true local S-commensurate orders.

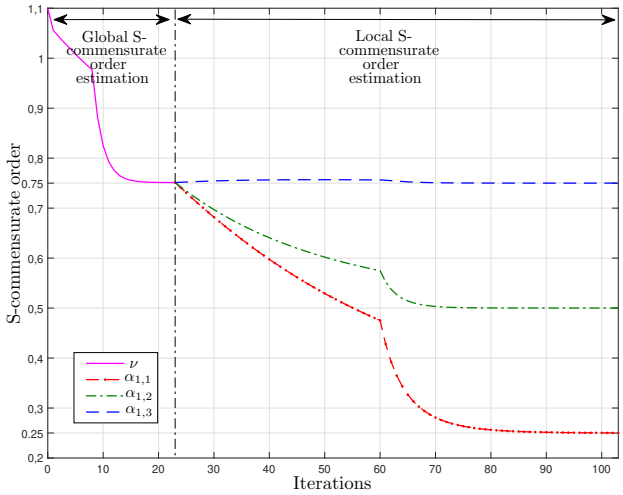

Fig. 4. S-commensurate order estimation versus number of iterations in example 2

4.4.2 *Example 3 — All differentiation order estimation combined with the srivcf algorithm*

Consider now the following MISO system where the commensurability constraint is released for all subsystems:

$$S_3 : \begin{cases} G_1(s) = \dfrac{1}{1 + 1.5s^{1.2} + 0.5s^{2.8}} \\ G_2(s) = \dfrac{0.5}{1 + 1.5s^{1.1} + 0.4s^{2.5}} \\ G_3(s) = \dfrac{1.5}{1 + 1.5s^{0.7} + 0.6s^{1.6}}. \end{cases} \tag{59}$$

The input signals plotted in Fig.2, are again used for system identification. The noise-free output $y(t)$, is corrupted by a zero mean Gaussian white noise, with a greater noise level NSR $= -10$dB, and the sampling period is set to $T = 0.2s$.

The model structure is set, as the true one, to:

$$G_k = \frac{b_{0,k}}{1 + a_{1,k}s^{\alpha_{1,k}} + a_{2,k}s^{\alpha_{2,k}}}, \text{ for } k = 1,\ 2,\ 3. \tag{60}$$

The goal is to estimate all the differentiation orders along with all the coefficients of the three subsystems.

Fig. 5 illustrates the evolution of all differentiation order estimation. In the first stage, a global S-commensurate order ν (—) is estimated; then local S-commensurate orders are estimated in the second stage ($\nu_1 = \alpha_{1,1}$ for G_1 (– –), $\nu_2 = \alpha_{1,2}$ for G_2(– -) and $\nu_3 = \alpha_{1,3}$ for G_3(–*–)). Finally, at the last stage, the S-commensurability constraint is released and all differentiation orders are well estimated.

At this third stage, after the local S-commensurate order estimation (at iteration 41 in Fig. 5), when releasing the

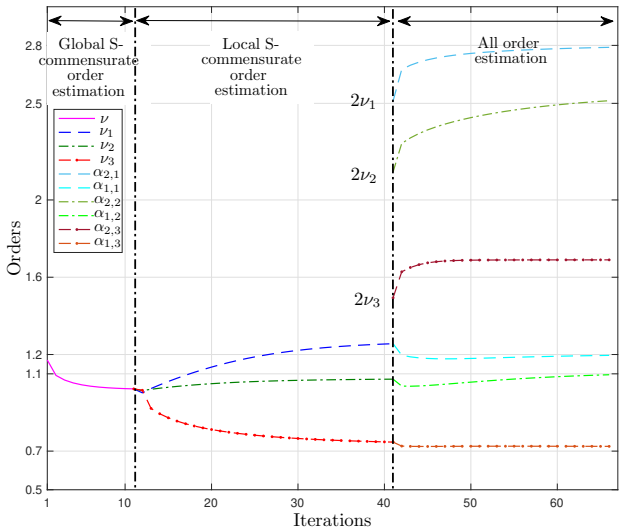

Fig. 5. Differentiation order estimation versus number of iterations in example 3

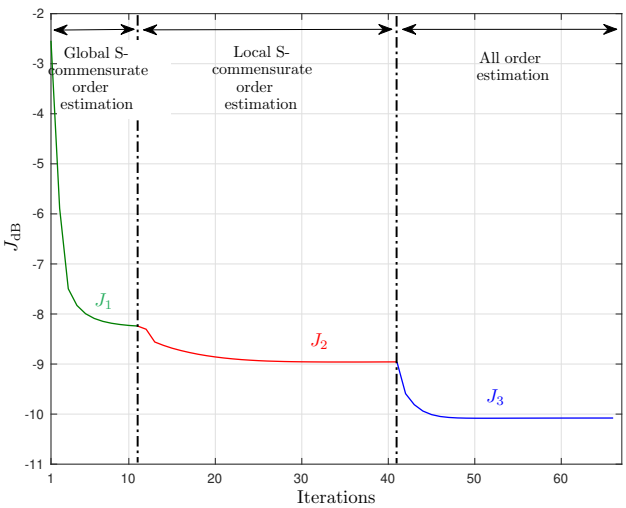

Fig. 6. Cost function versus iteration number in example 3

S-commensurability constraint, the immediate following differentiation orders are fixed to the double of the local S-commensurate order: $\alpha_{2,1} = 2 \times \nu_1$, $\alpha_{2,2} = 2 \times \nu_2$ and $\alpha_{2,3} = 2 \times \nu_3$.

Fig. 6 illustrates the criterion evolutions with respect to the three stages, and confirms that all parameters, as well the differentiation orders as the coefficients, have been correctly estimated with the full MISO-oosrivcf algorithm. Note that:

- for the first stage, when a global S-commensurate order is estimated for all subsystems, the cost function $J = -8.24$dB, so the ℓ_2-norm of the modeling error is around 1.76dB (see J_1 in Fig. 6);
- for the second stage when local S-commensurate orders are estimated, the cost function $J_{dB} = -8.96$dB, so the ℓ_2-norm of the modeling error has decreased to 1.04dB (see J_2 in Fig. 6);
- for the last stage, when all differentiation orders are estimated without any constraint, the cost function $J_{dB} = -10.08$dB, so the ℓ_2-norm of the modeling error is around zero dB (see J_3 in Fig. 6).

Table 3
Monte Carlo simulation with 50 runs for the estimation of differentiation orders and coefficients ($\bar{\theta}$ is the mean and $\hat{\sigma}(\theta)$ the standard deviation of the estimates) with NSR $= -10dB$

	True	MISO oosrivcf	
	θ	$\bar{\theta}$	$\hat{\sigma}_\theta$
$b_{0,1}$	1	1.0022	0.0194
$a_{1,1}$	1.5	1.4989	0.0351
$a_{2,1}$	0.5	0.5035	0.0286
$\alpha_{1,1}$	1.2	1.1952	0.0191
$\alpha_{2,1}$	2.8	2.7930	0.0277
$b_{0,2}$	0.5	0.5069	0.0332
$a_{1,2}$	1.5	1.4981	0.0927
$a_{2,2}$	0.4	0.4332	0.1022
$\alpha_{1,2}$	1.1	1.0797	0.0774
$\alpha_{2,2}$	2.5	2.4832	0.1743
$b_{0,3}$	1.5	1.4930	0.0567
$a_{1,3}$	1.5	1.5306	0.1367
$a_{2,3}$	0.6	0.5823	0.1315
$\alpha_{1,3}$	0.7	0.7242	0.0558
$\alpha_{2,3}$	1.6	1.6282	0.1209

A Monte Carlo simulation with different noise realizations with 50 runs has been carried out and the results are provided in table 3, with a mean value close to the true parameters and with a low estimation variance. The proposed MISO-oosrivcf algorithm for differentiation order and coefficient estimation is therefore validated in this example as the estimated parameters have converged to the true ones.

5 Conclusion

This paper has presented an optimal instrumental variable method for estimating transfer function coefficients of fractional MISO differential systems when the output is corrupted by an additive white noise. The well-known srivc (srivcf for fractional systems) algorithm has been extended for estimating transfer function coefficients of fractional MISO models when all differentiation orders are set according to prior knowledge. When the prior knowledge is not available, a two stage algorithm has been developed, which combines simultaneously the coefficient estimation through the MISO-srivcf algorithm and the differentiation order estimation through a gradient-based algorithm. Three variants have

been proposed: a global S-commensurate order is estimated for the whole fractional MISO system, or local S-commensurate orders are estimated for each subsystem, or even all differentiation orders are estimated without the commensurability constraint. An initialization procedure is proposed, consisting of estimating a global S-commensurate model first, then local S-commensurate orders, and finally all differentiation orders. The performances of the proposed algorithms have been evaluated by Monte Carlo simulation analysis. In a future work, it would be interesting to develop techniques to help fixing the number of parameters when the MISO model structure is not known. It will also be interesting to extend this study to deal with colored output noise by using hybrid Box–Jenkins MISO models with continuous-time fractional input–output models and discrete-time noise models. A further extension of the MISO-oosrivcf algorithm could tackle parametric identification with time-delays.

References

[1] E.W. Bai. An optimal two stage identification algorithm for Hammerstein-Wiener nonlinear systems. *Automatica*, 34(3):333–338, 1998.

[2] A. Benchellal, S. Bachir, T. Poinot, and J.-C. Trigeassou. Identification of a non-integer model of induction machines. In *1st IFAC Workshop on Fractional Differentiation and its Applications (FDA)*, pages 400–407, Bordeaux, France, 2004.

[3] F. Chen, H. Garnier, M. Gilson, and X. Zhuan. Frequency domain identification of continuous-time output-error models with time-delay from relay feedback tests. *Automatica*, 98:180–189, 2018.

[4] M. Chetoui, M. Thomassin, R. Malti, M. Aoun, S. Najar, M. N. Abdelkrim, and A. Oustaloup. New consistent methods for order and coefficient estimation of continuous-time errors-in-variables fractional models. *Computers & Mathematics with Applications*, 66(5):860 – 872, 2013. Fractional Differentiation and its Applications.

[5] O. Cois, A. Oustaloup, T. Poinot, and J.-L. Battaglia. Fractional state variable filter for system identification by fractional model. In *6th European Control Conference ECC'01*, Porto, Portugal, 2001.

[6] T. Djamah, R. Mansouri, S. Djennoune, and M. Bettayeb. Optimal low order model identification of fractional dynamic systems. *Applied Mathematics and Computation*, 206(2):543–554, 2008.

[7] J.-D. Gabano and T. Poinot. Estimation of thermal parameters using fractional modelling. *Signal Processing*, 91(4):938 – 948, 2011.

[8] F. Gao, X. J. Lee, F. X. Fei, H. Q. Tong, Y. F. Deng, and H. L. Zhao. Identification time-delayed fractional order chaos with functional extrema model via differential evolution. *Expert Systems with Applications*, 41(4):1601–1608, 2014.

[9] Z. Gao, X. Lin, and Y. Zheng. System identification with measurement noise compensation based on polynomial modulating function for fractional-order systems with a known time-delay. *ISA transactions*, 79:62–72, 2018.

[10] H. Garnier, M. Gilson, P.C. Young, and E. Huselstein. An optimal IV technique for identifying continuous-time transfer function model of multiple input systems. *Control Engineering Practice*, 15(4):471–486, 2007.

[11] H. Garnier and L. Wang. *Identification of continuous-time models from sampled data.* Springer-Verlag, 2008.

[12] T.T. Hartley, C.F. Lorenzo, J.-C. Trigeassou, and N. Maamri. Equivalence of history-function based and infinite-dimensional-state initializations for fractional-order operators. *ASME Journal of computational and nonlinear dynamics*, 8(4):041014–041014–7, 2013.

[13] T. Higo, T. Kawaguchi, M. Itamoto, and S. Adachi. Recursive identification of fractional time-delay systems using discrete-time model. *IFAC-PapersOnLine*, 51(15):939–944, 2018.

[14] C. M. Ionescu and R. De Keyser. Relations between fractional-order model parameters and lung pathology in chronic obstructive pulmonary disease. *IEEE Transactions on Biomedical Engineering*, 56(4):978–987, 2009.

[15] L. I. Jing and G. U. O. Boling. Parameter identification in fractional differential equations. *Acta Mathematica Scientia*, 33(3):855–864, 2013.

[16] S.M. Kay. *Fundamentals of statistical signal processing: estimation theory.* Prentice-Hall, Upper Saddle River, NJ, 1993.

[17] V. Laurain, R. Toth, M. Gilson, and H. Garnier. Identification of input-output lpv models. In *Linear parameter-varying system identification: new developments and trends*, pages 95–131. World Scientific, 2012.

[18] G. Liu, L. Wang, W. L. Luo, J. K. Liu, and Z. R. Lu. Parameter identification of fractional order system using enhanced response sensitivity approach. *Communications in Nonlinear Science and Numerical Simulation*, 67:492–505, 2019.

[19] L. Ljung. *System identification – Theory for the user.* Prentice-Hall, Upper Saddle River, N.J., USA, 2 edition, 1999.

[20] L. Ljung, T. Chen, and B. Mu. A shift in paradigm for system identification. *International Journal of Control*, 93(2):173–180, 02 2020.

[21] C. Lorenzo and T. Hartley. Initialization of fractional-order operators and fractional differential equations. *Journal of computational and nonlinear dynamics. Special issue on discontinuous and fractional dynamical systems*, 3:021101–1,021101–9, April 2008.

[22] A. Maachou, R. Malti, P. Melchior, J.-L. Battaglia, A. Oustaloup, and B Hay. Nonlinear thermal system identification using fractional Volterra series. *Control Engineering Practice*, 29:50–60, 2014.

[23] R. L. Magin. Fractional calculus models of complex dynamics in biological tissues. *Comput. Math. Appl.*, 59:1586–1593, March 2010.

[24] R. Malti, S. Victor, and A. Oustaloup. Advances in system identification using fractional models. *Journal of Computational and Nonlinear Dynamics*, 3:021401.1–021401.7, 2008.

[25] R. Mansouri, M. Bettayeb, and S. Djennoune. Multivariable fractional system approximation with initial conditions using integral state space representation. *Computers & Mathematics with Applications*, 59(5):1842 – 1851, 2010.

[26] D. Matignon. Stability properties for generalized fractional differential systems. *ESAIM proceedings - Systèmes Différentiels Fractionnaires - Modèles, Méthodes et Applications*, 5, 1998.

[27] S. Mukhopahyay, A. Patra, and G. P. Rao. Irreducible model estimation for MIMO systems. *International Journal of Control*, 53(1):223–253, 1991.

[28] A. Narang, S.L. Shah, and T. Chen. Continuous-time model identification of fractional-order models with time delays. *IET Control Theory & Applications*, 5(7):900–912, 2011.

[29] A. Nasser-Eddine, B. Huard, J. D. Gabano, T. Poinot, S. Martemianov, and A. Thomas. Fast time domain identification of electrochemical systems at low frequencies using fractional modeling. *Journal of Electroanalytical Chemistry*, 862:113957, 2020.

[30] A. Oustaloup. *La dérivation non-entière : théorie, synthèse et applications*. Hermès, Paris, 1995.

[31] A. Oustaloup. *Diversity and Non-integer Differentiation for System Dynamics*. Wiley-ISTE, 2014.

[32] S. Pan, R.A. González, J.S. Welsh, and C. R. Rojas. Consistency analysis of the simplified refined instrumental variable method for continuous-time systems. *Automatica*, 113:108767, 2020.

[33] V. Pascu, H. Garnier, L. Ljung, and A. Janot. Benchmark problems for continuous-time model identification: Design aspects, results and perspectives. *Automatica*, 107:511–517, 2019.

[34] G. Pillonetto, F. Dinuzzo, T. Chen, G. De Nicolao, and L. Ljung. Kernel methods in system identification, machine learning and function estimation: A survey. *Automatica*, 50(3):657–682, 2014.

[35] I. Podlubny. *Fractional Differential Equations: An Introduction to Fractional Derivatives, Fractional Differential Equations, to Methods of Their Solution and Some of Their Applications*. Academic Press, San Diego, 1999.

[36] G.P. Rao and H. Unbehauen. Identification of continuous-time systems. *Electrical Engineering*, 153:185 – 220, 2006.

[37] T. Söderström and P. Stoica. *Instrumental variable methods for system identification*. Springer Verlag, New York, 1983.

[38] W. Spinelli, L. Piroddi, and M. Lovera. A two-stage algorithm for structure identification of polynomial NARX models. *American Control Conference Vols 112*, 1-12:2387–2392, 2006.

[39] P. Stoica and R. Moses. *Spectral Analysis of Signals*. Pearson Prentice-Hall, Upper Saddle River, NJ, 2005.

[40] Y. Tang, H. Liu, W. Wang, Q. Lian, and X. Guan. Parameter identification of fractional order systems using block pulse functions. *Signal Processing*, 107:272 – 281, 2015.

[41] M. Thomassin and R. Malti. Subspace method for continuous-time fractional system identification. *IFAC Proceedings Volumes - 15th IFAC Symposium on System Identification (SYSID'2009)*, 42(10):880–885, 2009.

[42] J. C. Trigeassou and N. Maamri. Initial conditions and initialization of linear fractional differential equations. *Signal Processing*, 91(3):427–436, 2011.

[43] S. Victor, R. Malti, H. Garnier, and A. Oustaloup. Parameter and differentiation order estimation in fractional models. *Automatica*, 49(4):926–935, 2013.

[44] S. Victor, P. Melchior, M. Pellet, and A. Oustaloup. Lung thermal transfer system identification with fractional models. *IEEE Transactions on Control Systems Technology*, 28(1):172–182, 2020.

[45] J. Wang, W. X. Zheng, and T. Chen. Identification of linear dynamic systems operating in a networked environment. *Automatica*, 45(12):2763–2772, 2009.

[46] L.-Y. Wang and W.-X. Zhao. System identification: New paradigms, challenges, and opportunities. *Acta Automatica Sinica*, 39(7):933–942, 2013.

[47] Y. Wang, M. Li, and Z. Chen. Experimental study of fractional-order models for lithium-ion battery and ultra-capacitor: Modeling, system identification, and validation. *Applied Energy*, 278:115736, 2020.

[48] P.C. Young. An instrumental variable method for real-time identification of a noisy process. *Automatica*, 6:271–287, 1970.

[49] P.C. Young. Parameter estimation for continuous-time models – a survey. *Automatica*, 17(1):23–29, 1981.

[50] P.C. Young. Optimal IV identification and estimation of continuous-time TF models. In *15th World IFAC Congress*, Barcelona (Spain), 2002. IFAC, Elsevier.

[51] P.C. Young, H. Garnier, and M. Gilson. Identification of continuous-time models from sampled data. In H. Garnier and L. Wang, editors, *Identification of continuous-time models from sampled data*, chapter Refined Instrumental Variable Identification of Continuous-time Hybrid Box-Jenkins Models, pages 91–131. Springer-Verlag, 2008.

[52] P.C. Young and A.J. Jakeman. Refined instrumental variable methods of time-series analysis: Part III, extensions. *International Journal of Control*, 31:741–764, 1980.